


## ABSORPTION AND DISTRIBUTION OF ULTRATRACE EXOGENOUS <sup>14</sup>C UREA IN RATS

Li Wang<sup>1,2</sup> • Hongtao Shen<sup>1\*</sup>  • Junsen Tang<sup>1</sup> • Guofeng Zhang<sup>1</sup> • Linjie Qi<sup>1</sup> • Dingxiong Chen<sup>1</sup> • Kaiyong Wu<sup>1</sup> • Xinyi Han<sup>1</sup> • He Ouyang<sup>1</sup> • Yun He<sup>1</sup> • Pucheng Yang<sup>3</sup> • Xue Zhang<sup>3</sup> • Chunbo Xia<sup>3</sup>

<sup>1</sup>Guangxi Key Laboratory of Nuclear Physics and Technology, Guangxi Normal University, Guilin 541004, China

<sup>2</sup>School of Physics, Hubei University, Wuhan Hubei 430062, China

<sup>3</sup>Guilin Medical University, Guilin 541004, China

**ABSTRACT.** The absorption and distribution of radiocarbon-labeled urea at the ultratrace level were investigated with a <sup>14</sup>C-AMS biotracer method. The radiopharmaceutical concentrations in the plasma, heart, liver, spleen, lung, kidney, stomach, brain, bladder, muscle, testis, and fat of rats after oral administration of <sup>14</sup>C urea at ultratrace doses were determined by AMS, and the concentration-time curves in plasma and tissues and pharmacokinetic distribution data were obtained. This study provides an analytical method for the pharmacokinetic parameters and tissue distribution of exogenous urea in rats at ultratrace doses and explores the feasibility of evaluation and long-term tracking of ultratrace doses of drugs with AMS.

**KEYWORDS:** accelerator mass spectrometry, <sup>14</sup>C urea, distribution, pharmacokinetics, ultratrace.

### INTRODUCTION

Accelerator mass spectrometry (AMS) is a technology with an extremely high isotope detection sensitivity. Compared with conventional detection methods, it has the advantages of a short measurement time, small sample amount, and high measurement sensitivity (Bennett et al. 1997; Nelson et al. 1977). As the most sensitive method for measuring <sup>14</sup>C, the method is widely used in archaeology, environmental science, geology, oceanography, biomedicine, and other fields (Nielsen, 1952; Lubritto et al. 2004; Marzaioli et al. 2005; Mary et al. 2011; Salehpour et al. 2015; Cheng et al. 2019). Since the U.S. Food and Drug Administration (FDA) has used the pharmacokinetic data of radioisotope-labeled drugs as an essential basis for the safety evaluation of new drugs and formulated corresponding regulations (FDA, 2010), similar regulations have also been formulated around the world for the early development and the later application of drugs. Therefore, radioactive tracer technology has been used in more than 80% of drugs to investigate absorption, distribution, metabolism, and excretion (Lappin and Garner, 2005).

The main detection methods used in isotope tracing technology include liquid scintillation (LSC) (L'Annunziata and Kessler, 1998), autoradiography (ARG) (Partridge et al. 2008), and positron emission computerized tomography (PET) (Li et al. 2010). The miniaturization of PET and the development of QWBA technology have made the localization of radiolabeled drugs in organisms easier and more intuitive (Li et al. 2008; Weiss et al. 2007; D'souza et al. 2007). However, due to the limitation of measurement sensitivity, conventional detection techniques cannot measure ultratrace doses of drugs or track radiolabeled drugs for a long time (Lappin and Garner, 2003). On the other hand, the high sensitivity and extremely low detection limit of AMS technology allows the administration of subpharmacological doses of radiolabeled drugs to animals or humans at radiologically unremarkable levels to obtain preliminary information on drug absorption, distribution, metabolism, and excretion and has been increasingly valued by the pharmaceutical industry (Sandhu, 2004). To date, most studies on the metabolism and treatment of exogenous organisms in AMS have focused on the

\*Corresponding author. Email: [shenht@gxnu.edu.cn](mailto:shenht@gxnu.edu.cn)

combination of carcinogens with DNA and proteins (Turteltaub et al. 1990, 1997), and there are fewer studies in the pharmaceutical field under the conditions of ultratrace dose administration and subpharmacological doses (Kaye et al. 1997; Young et al. 2008).

In our study, AMS technology was used to measure the absorption and distribution of  $^{14}\text{C}$  urea in rats treated with ultratrace doses, verify the feasibility of AMS technology in ultratrace dose drug research and long-term drug tracking at the technical level, and assess the pharmacokinetic characteristics of the drug, which provides a reference for the use of AMS technology in the evaluation of ultratrace-dosing drug research and research on human subjects.

## MATERIALS AND METHODS

### Chemicals

$^{14}\text{C}$  urea capsules (SFDA #H20000020) were obtained from Shenzhen Zhonghe Headway Biotechnology Co., Ltd., China, CuO powder (GB/T674-2003, purity:  $\geq 99.0\%$ ) was obtained from Sinopharm Chemical Reagent Co., Ltd., Fe powder (#209309, 325 mesh, 97%) was obtained from Sigma–Aldrich USA, and Zn powder (#324930,  $<150\ \mu\text{m}$ , 99.995%) was obtained from Sigma–Aldrich USA.

### Dosage

$^{14}\text{C}$  urea was dissolved in distilled water at a dose of  $4.302 \times 10^{-7}\ \text{mg/mL}$ . The oral dose administered to rats was  $2.044 \times 10^{-6}\ \text{mg/kg}$  bdw (body weight), and the radioactive dose was  $2.058 \times 10^{-3}\ \mu\text{Ci/kg}$  bdw, six orders of magnitude lower than the conventional dose (Nomura et al. 2006; Park et al. 2012).

### Animals

Twenty-four male Sprague–Dawley rats (SPF, Guilin Medical College, Guilin, China) weighing 243–370 g were used.

### Animal Experiment

Rats were kept in individual metabolism cages in a room with a temperature of  $21^\circ\text{C}$ – $25^\circ\text{C}$  and humidity of 50–60% with a daily light/dark schedule of 12/12 hr, with free access to water throughout acclimatization. Food was removed for 12 rh before experiments and for an additional 12 hr after administration of  $^{14}\text{C}$  urea. Intra-gastric administration was performed at doses of  $2.044 \times 10^{-6}\ \text{mg/kg}$  bdw ( $2.058 \times 10^{-3}\ \mu\text{Ci/kg}$  bdw) with a stomach tube. The sampling time was 0.25 hr, 0.5 hr, 1 hr, 4 hr, 8 hr, 24 hr, and 72 hr, and 3 rats were dissected and sampled at each sampling time (the method of sacrifice was spinal dislocation) for collection of biological samples such as plasma, heart, liver, spleen, lung, kidney, stomach, brain, bladder, fat, muscle, and gonads. A blank control group (3 rats, no drug) was used for comparison. All experiments were conducted in accordance with the ethical guidelines of the Ministry of Health of China.

### Sample Preparation for AMS Measurement

The collected biological samples were packed into 3–20 mL glass vials and placed in a vacuum lyophilizer for a 48 hr drying process at  $-70^\circ\text{C}$ , after which the samples were ground and stored at  $-20^\circ\text{C}$ . The carbon content of plasma and various blank tissue samples was measured by an elemental analyzer (manufacturer: Elementar, model: UNICUBE). The biological sample



Figure 1 A glass vacuum line for graphite preparation.

containing 1 mg of carbon was mixed with CuO powder (pretreatment at 900°C for 3 hr) at a ratio of 1:40 in the combustion tube in the vacuum sample preparation device for evacuation, as shown in Figure 1 (Shen et al. 2022a, 2022b). The combustion tube was sealed with a flame after the vacuum was lower than  $5 \times 10^{-4}$  mbar and placed in a muffle furnace at 900°C for 3 hr to fully react with the sample and generate CO<sub>2</sub>. Then, the combustion tube was crushed in a crushing device of the vacuum line. The CO<sub>2</sub> gas first passed through the alcohol liquid nitrogen cold traps at -90°C to thoroughly remove the water vapor and then entered the liquid nitrogen cold trap at -196°C, where it was frozen. Any noncondensable gases, such as SO<sub>2</sub>, N<sub>2</sub>, and O<sub>2</sub>, were pumped away. The purified CO<sub>2</sub> was heated, transferred to a reduction tube using a liquid nitrogen cold trap, and finally sealed with a torch. The reduction tube was preloaded with 15–25 mg Zn powder and 2.5–3.0 mg Fe powder and pretreated at 400°C for 3 hr. The reduction tube was then subjected to reduction treatment in the graphite reduction furnace at 650°C for 8 hr so that the CO<sub>2</sub> reacted with Zn to produce graphite on the surface of Fe (Jull et al. 1986; Slota et al. 1987), as shown in Figure S1. Finally, the graphite and Fe powder were pressed into the AMS cathodes for measurement.

### Measurement of Radioactivity

The GXNU-AMS instrument (Shen et al. 2022a, 2022b) was mainly composed of a cesium negative ion sputtering source, preacceleration line, injection magnet, main acceleration line, gas stripper, analysis magnet, electrostatic analyzer, and detector, as shown in Figure S2. The processed blank samples, experimental samples, and standard samples (OX-II, IAEA-C8, IAEA-C1) were installed in the cathode wheel of the ion source, as shown in Figure S3. The negative ion beam C<sup>-</sup> was extracted from the ion source and then entered a double-focusing dipole injection magnet through a preacceleration tube for mass selection. An alternating high-frequency potential (Trek 10/10B-HS) was applied to the vacuum box in the injection magnet for the high-speed alternating injection of C isotopes <sup>12</sup>C<sup>-</sup>, <sup>13</sup>C<sup>-</sup>, and <sup>14</sup>C<sup>-</sup>, which were focused by an electric quadrupole triplet lens and then accelerated into the gas stripper through a 150-kV accelerating tube. He in the gas stripper stripped and converted the negatively charged

ions into neutral or positive charge states, while the negative molecular ions ( $^{12}\text{CH}_2^-$ ,  $^{13}\text{CH}^-$ , etc.) were dissociated into their component atoms, which entered the analysis magnet at the high energy end for ion momentum/charge selection, then via the electrostatic analyzer for ion energy/charge selection to eliminate various scattered particles. Finally, the pure  $^{14}\text{C}^+$  entered the end detector for counting. In addition,  $^{12}\text{C}$  and  $^{13}\text{C}$  beam values were recorded in Faraday cups at the low and high energy sides for isotope fractionation correction and  $^{14}\text{C}/^{12}\text{C}$  abundance calculation of the samples. The measured values of the biological samples were calibrated with the standard samples, and then the drug concentration was analyzed by Equation (1).

$$C = R_{\frac{^{14}\text{C}}{^{12}\text{C}}} \times P / B \quad (1)$$

where  $C$  is the  $^{14}\text{C}$  urea concentration in plasma and tissues,  $R$  is the abundance ratio of  $^{14}\text{C}/^{12}\text{C}$ ,  $P$  is the content of carbon in the plasma or tissue, and  $B$  is the content of carbon in urea.

## RESULTS AND DISCUSSION

### Carbon Recovery from the Biological Sample

Similar to the methods described by Walker et al. (2019) and Orsovszki et al. (2015), a temperature gradient was applied to the graphite reduction process. The Fe and Zn catalysts were held at high reaction temperatures ( $\sim 600^\circ\text{C}$ ), whereas the tops of the Zn tube reactors were held at ambient temperatures ( $20\text{--}25^\circ\text{C}$ ). The gaseous Zn and ZnO generated during the reaction process were sequentially condensed on the cooler part (between  $450^\circ\text{C}$  and room temperature) of the reduction tube, as shown in Figure S4, to avoid condensation on the surface of Fe powder affecting the sample purity and improve the graphite synthesis efficiency. The average graphite recovery rate treated by this method was approximately 90% with a small fluctuation (Figure 2), which proves the stability and reliability of our vacuum  $^{14}\text{C}$  preparation device.

### Carbon Content of Plasma and Tissues

The biocarbon contents of the vacuum-dried plasma and tissue samples were measured with the CHNS mode of the elemental analyzer (Elemental UNICUBE), similar to the method described by Lappin and Garner (2005), which was used to calculate the drug concentration of  $^{14}\text{C}$  urea. The measurement results are shown in Table 1.

### $^{14}\text{C}$ Urea Concentrations in Plasma

The relationship between the radiopharmaceutical concentration in plasma and time following oral administration of  $^{14}\text{C}$  urea is shown in Figure 3. The metabolic data were pharmacokinetically processed using Phoenix Winnonlin 8.1 (Certara, USA) software (Schütz, 2012), as shown in Table 2. The rapid peak time of  $^{14}\text{C}$  urea absorption was only 0.25 hr, with a peak concentration of  $1.323 \times 10^{-3}$  ng/mL, an average retention time of 23.49 hr, a steady-state distribution volume of 3.403 mL/kg, and a clearance rate of 79.95 mL/h/kg.

### $^{14}\text{C}$ Urea Distribution in Tissues

The measurement data of the radiopharmaceutical concentration in different tissues of rats at 0.25 hr, 0.5 hr, 1 hr, 4 hr, 8 hr, 24 hr, and 72 hr after oral administration of  $^{14}\text{C}$  urea are shown

Table 1 Biological C, H, N, and S content in dried plasma and tissues.

Tissue	Carbon content (%)	Hydrogen content (%)	Nitrogen content (%)	Sulfur content (%)
Plasma	42.92 ± 0.02	6.37 ± 0.01	12.83 ± 0.01	0.884 ± 0.001
Heart	45.21 ± 0.07	6.91 ± 0.01	12.13 ± 0.02	1.509 ± 0.001
Liver	47.09 ± 0.04	7.14 ± 0.01	11.00 ± 0.01	1.076 ± 0.001
Spleen	42.97 ± 0.05	6.52 ± 0.01	11.33 ± 0.01	0.968 ± 0.001
Lung	48.81 ± 0.03	7.62 ± 0.01	9.72 ± 0.01	0.857 ± 0.001
Kidney	44.52 ± 0.03	6.97 ± 0.01	10.97 ± 0.01	0.987 ± 0.001
Stomach	42.57 ± 0.05	6.85 ± 0.01	11.22 ± 0.01	0.981 ± 0.001
Brain	50.95 ± 0.07	7.71 ± 0.01	7.84 ± 0.01	0.766 ± 0.001
Bladder	41.28 ± 0.05	6.68 ± 0.01	12.18 ± 0.01	0.785 ± 0.001
Fat	56.41 ± 0.04	8.77 ± 0.01	1.93 ± 0.01	0.412 ± 0.001
Muscle	43.36 ± 0.02	6.71 ± 0.01	13.18 ± 0.01	1.107 ± 0.002
Testicle	43.69 ± 0.03	6.88 ± 0.01	11.39 ± 0.01	0.999 ± 0.001

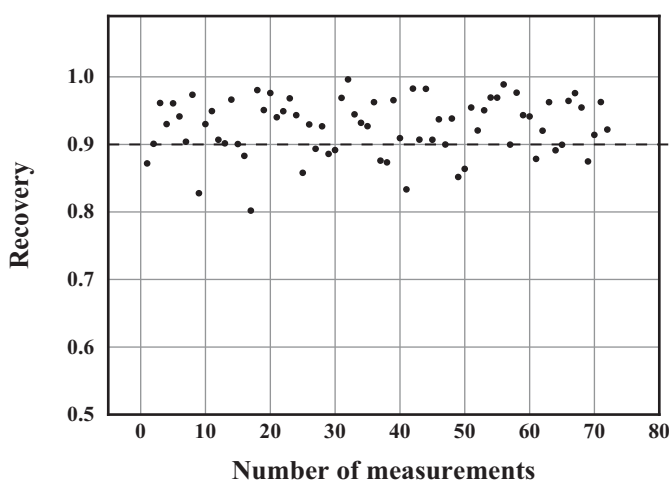


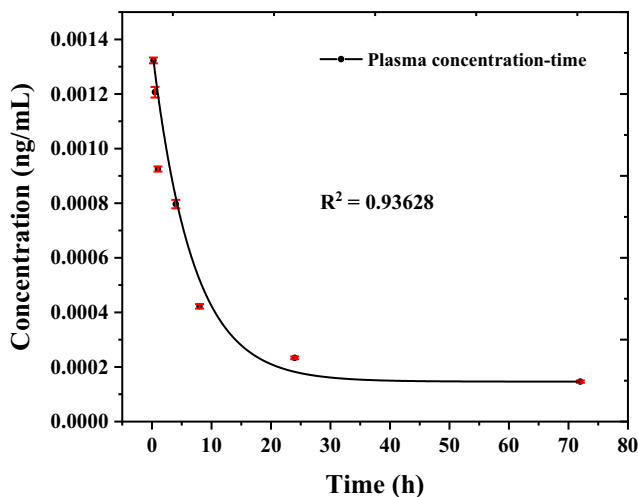
Figure 2 Graphite recovery of biological samples.

in Table 3, Figure 4, and Figure S5. As shown in the data, the presence of  $^{14}\text{C}$  urea was detected in all 11 tissues and plasma, with the radiopharmaceutical concentration peaking at 0.25 hr in plasma and liver, at 0.5 hr in heart, spleen, lung, kidney, stomach, bladder, fat, and muscle, and at 4 hr in brain and testis.

The radiopharmaceutical concentrations in the heart, liver, spleen, lung, kidney, stomach, bladder, fat, muscle, and testis were higher than that in plasma, and the peak value of concentration in each organ concentration was  $4.987 \times 10^{-3}$  ng/g,  $4.551 \times 10^{-3}$  ng/g,  $6.060 \times 10^{-3}$  ng/g,  $4.263 \times 10^{-3}$  ng/g,  $3.159 \times 10^{-2}$  ng/g,  $1.296 \times 10^{-2}$  ng/g,  $3.324 \times 10^{-3}$  ng/g,  $2.456 \times 10^{-2}$  ng/g,  $5.612 \times 10^{-3}$  ng/g,  $3.665 \times 10^{-3}$  ng/g, and  $9.418 \times 10^{-3}$  ng/g, respectively, which is similar to the distribution of urea in rats at conventional doses (Nomura et al. 2006; Park et al. 2012). The

Table 2 Pharmacokinetic parameters of  $^{14}\text{C}$ -urea determined by accelerator mass spectrometry after oral administration in fasted rats.

Parameters	Oral
Dose (mg/kg)	$2.044 \times 10^{-6}$
$C_{\max}$ (ng/mL)	$1.323 \times 10^{-3}$
$T_{\max}$ (h)	$2.500 \times 10^{-1}$
$\text{AUC}_{0-t}$ (ng·h/mL) <sup>a</sup>	$2.040 \times 10^{-2}$
$\text{AUC}_{0-\infty}$ (ng·h/mL)	$2.556 \times 10^{-3}$
MRT (h)	$23.49 \times 10^2$
$\text{Vd}_{\text{ss}}$ (l/kg) <sup>b</sup>	$3.403 \times 10^0$
$\text{CL}_t$ (mL/h/kg) <sup>c</sup>	$79.95 \times 10^2$

Figure 3 Radiopharmaceutical concentrations in plasma of rats after oral administration of  $^{14}\text{C}$  urea.

order of the radiopharmaceutical concentration in each tissue was kidney > bladder > stomach > testis > spleen > fat > heart > liver > lung > muscle > brain.

The radiopharmaceutical concentrations in the stomach, kidney, and bladder were much higher than those in other tissues, suggesting that urinary excretion is a major excretion route for  $^{14}\text{C}$  urea, which is similar to the metabolic trend of urea at conventional doses (Nomura et al. 2006; Park et al. 2012; Dickerson et al. 2018; Rapoport et al. 1982; Juhr et al. 1987, 1990). Drug concentrations in the brain, fat, and muscle were low, indicating that  $^{14}\text{C}$  urea did not easily enter highly lipidic tissues. The radiopharmaceutical concentration in the plasma decreased continuously from 0.25 hr to 72 hr, the radiopharmaceutical concentrations in all tissues were at a low level 24 hr after administration, and most of the drug and metabolites had been eliminated from the body. The measured radiopharmaceutical concentrations in plasma and tissue dropped to background levels at 72 hr, and no specific tissue accumulation of urea was detected.

Table 3  $^{14}\text{C}$ -urea concentrations in tissues after oral administration in fasted rats.

Tissue	Concentration ( $10^{-4}\text{ng/mL}^{\text{a}}$ or $10^{-4}\text{ng/g}$ )						
	0.25 hr	0.5 hr	1 hr	4 hr	8 hr	24 hr	72 hr
Plasma <sup>a</sup>	13.23 ± 0.11	12.06 ± 0.19	9.25 ± 0.09	7.97 ± 0.16	4.22 ± 0.08	2.34 ± 0.05	1.47 ± 0.04
Heart	47.17 ± 0.49	49.87 ± 0.96	35.26 ± 0.71	35.14 ± 0.84	14.48 ± 0.26	7.83 ± 0.20	6.09 ± 0.20
Liver	45.51 ± 0.53	40.25 ± 1.42	26.28 ± 0.53	13.19 ± 0.21	12.89 ± 0.18	10.85 ± 0.21	10.66 ± 0.27
Spleen	40.57 ± 0.58	60.60 ± 0.99	46.23 ± 1.62	45.74 ± 1.23	18.98 ± 0.43	16.37 ± 3.42	13.07 ± 0.20
Lung	13.43 ± 0.26	42.63 ± 0.17	32.22 ± 0.44	28.68 ± 0.63	14.49 ± 0.27	12.19 ± 0.41	9.90 ± 0.24
Kidney	12.67 ± 0.49	315.90 ± 0.63	94.18 ± 1.20	84.02 ± 1.31	22.22 ± 0.66	9.50 ± 0.19	8.30 ± 0.16
Stomach	18.67 ± 0.19	129.6 ± 1.35	64.54 ± 0.53	22.55 ± 0.64	20.68 ± 0.43	13.71 ± 0.20	10.75 ± 0.29
Brain	7.14 ± 0.11	11.21 ± 2.30	15.44 ± 0.41	33.24 ± 0.37	11.22 ± 0.79	9.01 ± 0.52	4.38 ± 0.11
Bladder	23.11 ± 0.42	245.6 ± 3.86	55.60 ± 0.64	24.82 ± 0.56	9.75 ± 0.05	2.60 ± 0.07	1.74 ± 0.03
Fat	21.40 ± 0.45	56.12 ± 1.37	33.44 ± 0.37	29.72 ± 0.53	23.85 ± 0.51	23.24 ± 0.32	16.00 ± 0.31
Muscle	18.51 ± 0.13	36.65 ± 0.67	29.00 ± 0.62	28.07 ± 0.50	11.61 ± 0.18	8.40 ± 0.19	8.12 ± 0.17
Testicle	28.12 ± 0.37	54.98 ± 0.93	70.47 ± 0.92	94.18 ± 1.37	39.85 ± 0.92	24.56 ± 0.51	18.27 ± 0.33

<sup>a</sup>The unit is only for plasma.

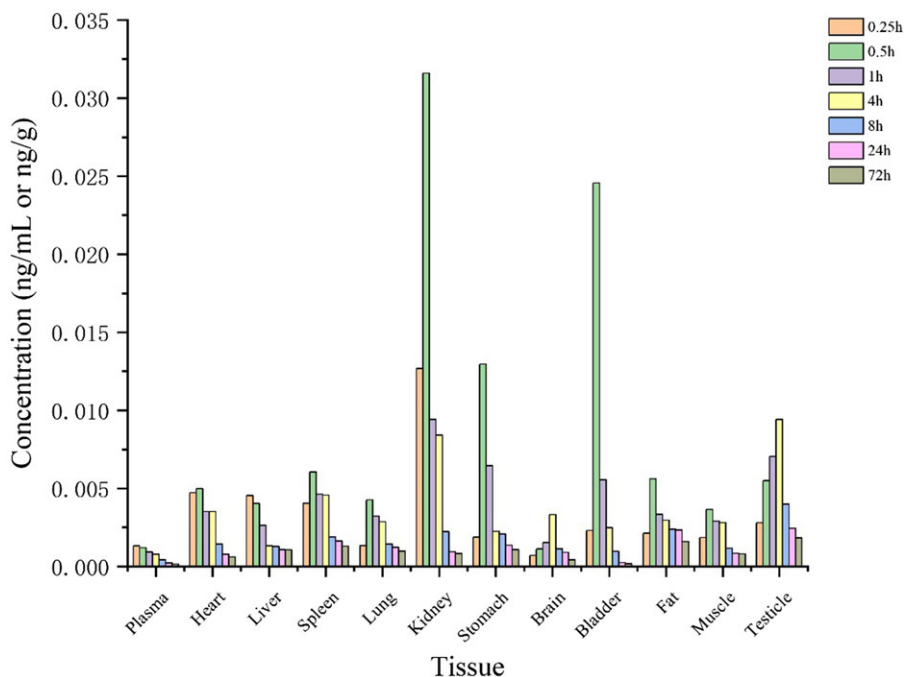


Figure 4  $^{14}\text{C}$ -urea concentrations in tissues of rats after oral administration of  $^{14}\text{C}$  urea.

## CONCLUSIONS

Ultratrace dose pharmacokinetic studies can provide pharmacokinetic parameters and distribution data beyond conventional doses, which play an essential role in the drug development process and help to select the most suitable drug for further clinical evaluation. In this study, we investigated the absorption and distribution of  $^{14}\text{C}$  urea at an oral ultratrace dose in various tissues of rats using AMS technique and obtained the first data on urea metabolism in the organism after an ultratrace dose.

The experimental results showed that after oral administration of  $2.044 \times 10^{-6}$  mg/kg ( $2.058 \times 10^{-3}$   $\mu\text{Ci/kg}$ )  $^{14}\text{C}$  urea, the presence of  $^{14}\text{C}$  urea was detected in all tissues. The radiopharmaceutical concentration reached a peak at 0.25 hr in plasma ( $1.323 \times 10^{-3}$  ng/mL) and at 0.5 hr in stomach and most tissues, which indicated that the oral absorption rate of urea is very fast. The radiopharmaceutical concentration in the kidney and bladder was high, and the peak concentration was much higher than in other tissues, which indicated that  $^{14}\text{C}$  urea at ultratrace doses is mainly excreted through the kidney-bladder and at a very rapid clearance rate of 79.95 mL/h/kg, which is consistent with the way by which conventional doses of urea are mainly excreted (Marshall et al. 1988). The low radiopharmaceutical concentration in the brain, fat, and muscle may be related to the plasma-brain barrier and the water solubility of urea, which is similar to the distribution of urea in rats and humans (Nomura et al. 2006; Park et al. 2012; Dickerson et al. 2018; Rapoport et al. 1982; Juhr et al. 1987, 1990). This distribution study of an ultratrace dose of  $^{14}\text{C}$  urea in rats has successfully demonstrated that AMS technology can be applied in the field of pharmacokinetics and radiopharmaceutical distribution research for ultratrace doses, which is difficult to achieve with traditional methods. The  $^{14}\text{C}$ -AMS technology developed in this work is expected to be a potential



analytical method for the long-term evaluation of pharmacokinetics and radiopharmaceutical distribution research and provide crucial scientific guidance for pharmacokinetics in human subjects.

## ACKNOWLEDGMENTS

This work was supported by the Central Government Guidance Funds for Local Scientific and Technological Development, China (No. Guike ZY22096024), the Guangxi Natural Science Foundation of China (No. 2017GXNSFFA198016), and the National Natural Science Foundation of China (Nos. 11775057, 11765004, and 12164006).

## SUPPLEMENTARY MATERIAL

To view supplementary material for this article, please visit <https://doi.org/10.1017/RDC.2024.47>

## REFERENCES

- Bennett CL, Beukens RP, Clover MR, et al. 1997. radiocarbon dating using electrostatic accelerators: negative ions provide the key. *Science* 198(4316): 508–510.
- Cheng P, Burr GS, Zhou W, et al. 2019. The deficiency of organic matter <sup>14</sup>C dating in Chinese Loess-paleosol sample. *Quaternary Geochronology* 56: 101051.
- D'Souza RA, Partridge EA, Roberts DW, et al. 2007. Distribution of radioactivity and metabolite profiling in tumor and plasma following intravenous administration of a colchicine derivative (14C - ZD6126) to tumor-bearing mice. *Xenobiotica* 37(3):328
- Dickerson AS, Lee JS, Keshava C, et al. 2018. Assessment of health effects of exogenous urea: summary and key findings. *Current Environmental Health Reports* 5(2):205–212.
- FDA, CDER, CBER. 2010. Draft Guidance for Industry: Investigational New Drug Applications (INDs)—Determining Whether Human Research Studies Can Be Conducted Without an IND.
- FDA, CDER, CBER. 2010. Guidance for Industry and Researchers: The Radioactive Drug Research Committee: Human Research Without An Investigational New Drug Application.
- Juhr NC, Franke J. 1987. [Metabolism of C14-labelled urea in conventional, germ-free and specifically associated rats]. *Zeitschrift für Versuchstierkunde* 29(3-4):157–164.
- Juhr NC, Franke J. 1990. Metabolism of <sup>14</sup>C-labeled urea in conventional and bacteria-free guinea pigs]. *Zeitschrift für Versuchstierkunde* 33(3):123.
- Jull AJT, Donahue DJ, Hatheway AL. 1986. Production of graphite targets by deposition from CO/H<sub>2</sub> for precision accelerator <sup>14</sup>C measurements. *Radiocarbon* 28(2A):191–197.
- Kaye B, Garner RC, Mauthe RJ, et al. 1997. A preliminary evaluation of accelerator mass spectrometry in the biomedical field. *Journal of Pharmaceutical & Biomedical Analysis* 16(3):541.
- L'Annunziata M, Kessler MJ. 1998. Handbook of radioactivity analysis. Academic Press.
- Lappin G, Garner RC. 2003. Ultra-sensitive detection of radiolabelled drugs and their metabolites using accelerator mass spectrometry. *Handbook of Analytical Separations* 4(03):331–349.
- Lappin G, Garner RC. 2005. The use of accelerator mass spectrometry to obtain early human ADME / PK data. *Expert Opin Drug Metab Toxicol* 1(1) : 23–31.
- Li Q, Xie L, Zhang J, et al. 2008. The distribution pattern of intravenous [<sup>14</sup>C] artesunate in rat tissues by quantitative whole-body autoradiography and tissue dissection techniques. *Journal of Pharmaceutical and Biomedical Analysis* 48(3): 876–884.
- Li Z, Conti PS. 2010. Radiopharmaceutical chemistry for positron emission tomography. *Advanced Drug Delivery Reviews* 62(11):1031–1051.
- Lubritto C, Rogalla D, Rubino M, et al. 2004. Accelerator mass spectrometry at the 4 MV Dynamitron Tandem in Bochum. *Nuclear Instruments & Methods in Physics Research* 255–260.
- Marshall BJ, Surveyor I. 1988. Carbon-14 urea breath test for the diagnosis of campylobacter pylori associated gastritis. *Journal of Nuclear Medicine* 29(1): 11.
- Mary, Pack A, Monica, et al. 2011. A method for measuring methane oxidation rates using lowlevels of <sup>14</sup>C-labeled methane and accelerator mass spectrometry. *Limnology and Oceanography: Methods* 9(6):245–260.
- Marzaioli F, Lubritto C, Battipaglia, et al. 2005. Reconstruction of past CO<sub>2</sub> concentration at a natural CO<sub>2</sub> vent site using radiocarbon dating of tree rings. *Radiocarbon* 47(2):257–263.

- Nelson DE, Korteling RG, Stott WR. 1977. Carbon-14: Direct Detection at Natural Concentrations. *Science* 198(4316):507–508.
- Nielsen ES. 1952. The use of radioactive carbon (C14) for measuring organic production in the sea. *ICES Journal of Marine Science* 18:117–140.
- Nomura N, Matsumoto S, et al. 2006. Disposition of exogenous urea and effects of diet in rats. *Arzneimittel-Forschung* 56(3):258–266.
- Orsovszki, G., & Rinyu, L.. (2015). Flame-sealed tube graphitization using zinc as the sole reduction agent: precision improvement of environmental <sup>14</sup>C measurements on graphite targets. *Radiocarbon*, 57(05), 979–990.
- Park SH, Dae HS, Han JC, et al. 2012. Pharmacokinetics and excretion into expired air of urea, a potential diagnosis reagent of helicobacter pylori infection. *Korean Journal of Clinical Pharmacy* 22(2):160–166.
- Partridge EA, D'Souza RA, Lenz EM, et al. 2008. Disposition and metabolism of the colchicine derivative [14C]-zd6126 in rat and dog. *Xenobiotica; the Fate of Foreign Compounds in Biological Systems* 38(4):399.
- Rapoport SI, Fitzhugh R, Pettigrew KD, et al. 1982. Drug entry into and distribution within brain and cerebrospinal fluid: [14C]urea pharmacokinetics. *American Journal of Physiology Regulatory Integrative & Comparative Physiology* 242(3):R339–R348.
- Salehpour M, Hakansson K, Possnert G. 2015. Small sample accelerator mass spectrometry for biomedical applications. *Nuclear Instruments and Methods in Physics Research, Section B. Beam Interactions with Materials and Atoms* 361: 43–47.
- Sandhu P. 2004. Evaluation of microdosing strategies for studies in preclinical drug development: demonstration of linear pharmacokinetics in dogs of a nucleoside analog over a 50-fold dose range. *Drug Metabolism & Disposition* 32(11): 1254–1259.
- Schütz H. 2012. Evaluation of replicate designs for (reference scaled) average bioequivalence according to FDA's guidances with Phoenix™ WinNonlin® (2012 Pharsight, A Certara Company, Tripos L.P.).
- Shen H, Tang J, Wang L, et al. 2022a. New sample preparation line for radiocarbon measurements at the GXNU Laboratory. *Radiocarbon* 64(6): 1501–1511.
- Shen H, Shi S, Tang J, et al. 2022b. <sup>14</sup>C-AMS technology and its applications to an oil field tracer experiment. *Radiocarbon* 64(5):1159–1169.
- Slota PJ, Jull AJT, Linick TW, et al. 1987. Preparation of small samples for <sup>14</sup>C accelerator targets by catalytic reduction of CO. *Radiocarbon* 29(2): 303–306.
- Turteltaub KW, Felton JS, Gledhill BL, et al. 1990. Accelerator mass spectrometry in biomedical dosimetry: relationship between low-level exposure and covalent binding of heterocyclic amine carcinogens to DNA. *Proceedings of the National Academy of Sciences of the United States of America* 87(14):5288–5292.
- Turteltaub KW, Mauthe RJ, Dingley KH, et al. 1997. MeIQx-DNA adduct formation in rodent and human tissues at low doses. *Mutat Res* 376(1–2): 243–252.
- Walker BD, Xu X. 2019. An improved method for the sealed-tube zinc graphitization of microgram carbon samples and C-14 AMS measurement. *Nuclear Instruments and Methods in Physics Research, Section B. Beam Interactions with Materials and Atoms* 438:58–65.
- Weiss HM, Wirz B, Schweitzer A, et al. 2007. ADME investigations of unnatural peptides: distribution of a <sup>14</sup>C-labeled β 3-Octaarginine in rats. *Chemistry & Biodiversity* 4(7):1413–1437.
- Young G, Ellis W, Ayrton J, et al. 2008. Accelerator mass spectrometry (AMS): recent experience of its use in a clinical study and the potential future of the technique. *Xenobiotica* 31(8–9):619–632.